Molecular Vision 2014; 20:561-574 <http://www.molvis.org/molvis/v20/561>
Received 30 May 2013 | Accepted 24 April 2014 | Published 26 April 2014

Retinal expression of the serine protease matriptase-2 (Tmprss6) and its role in retinal iron homeostasis

Jaya P. Gnana-Prakasam,[1] Renee B. Baldowski,[1] Sudha Ananth,[1] Pamela M. Martin,[1] Sylvia B. Smith,[2] Vadivel Ganapathy[1]

[1]*Department of Biochemistry and Molecular Biology, Medical College of Georgia, Georgia Regents University, Augusta, GA;* [2]*Department of Cellular Biology and Anatomy, Medical College of Georgia, Georgia Regents University, Augusta, GA*

Purpose: Matriptase-2 (also known as TMPRSS6) is a critical regulator of the iron-regulatory hormone hepcidin in the liver; matriptase-2 cleaves membrane-bound hemojuvelin and consequently alters bone morphogenetic protein (BMP) signaling. Hemojuvelin and hepcidin are expressed in the retina and play a critical role in retinal iron homeostasis. However, no information on the expression and function of matriptase-2 in the retina is available. The purpose of the present study was to examine the retinal expression of matriptase-2 and its role in retinal iron homeostasis.

Methods: RT–PCR, quantitative PCR (qPCR), and immunofluorescence were used to analyze the expression of matriptase-2 and other iron-regulatory proteins in the mouse retina. Polarized localization of matriptase-2 in the RPE was evaluated using markers for the apical and basolateral membranes. Morphometric analysis of retinas from wild-type and matriptase-2 knockout (*Tmprss6*$^{msk/msk}$) mice was also performed. Retinal iron status in *Tmprss6*$^{msk/msk}$ mice was evaluated by comparing the expression levels of ferritin and transferrin receptor 1 between wild-type and knockout mice. BMP signaling was monitored by the phosphorylation status of Smads1/5/8 and expression levels of Id1 while interleukin-6 signaling was monitored by the phosphorylation status of STAT3.

Results: Matriptase-2 is expressed in the mouse retina with expression detectable in all retinal cell types. Expression of matriptase-2 is restricted to the apical membrane in the RPE where hemojuvelin, the substrate for matriptase-2, is also present. There is no marked difference in retinal morphology between wild-type mice and *Tmprss6*$^{msk/msk}$ mice, except minor differences in specific retinal layers. The knockout mouse retina is iron-deficient, demonstrable by downregulation of the iron-storage protein ferritin and upregulation of transferrin receptor 1 involved in iron uptake. Hepcidin is upregulated in *Tmprss6*$^{msk/msk}$ mouse retinas, particularly in the neural retina. BMP signaling is downregulated while interleukin-6 signaling is upregulated in *Tmprss6*$^{msk/msk}$ mouse retinas, suggesting that the upregulaton of hepcidin in knockout mouse retinas occurs through interleukin-6 signaling and not through BMP signaling.

Conclusions: The iron-regulatory serine protease matriptase-2 is expressed in the retina, and absence of this enzyme leads to iron deficiency and increased expression of hemojuvelin and hepcidin in the retina. The upregulation of hepcidin expression in *Tmprss6*$^{msk/msk}$ mouse retinas does not occur via BMP signaling but likely via the proinflammatory cytokine interleukin-6. We conclude that matriptase-2 is a critical participant in retinal iron homeostasis.

Hepcidin is a small polypeptide hormone, consisting of 25 amino acids, that is obligatory for iron regulation [1,2]. Hepcidin is expressed predominantly in the liver. The peptide exhibits bactericidal activity at high non-physiologic concentrations; this coupled with the peptide's hepatic origin was the basis of the name "hepcidin" for the peptide and hepatic antimicrobial peptide (*HAMP* HGNC ID: 15595; OMIM: 606464) for the gene [3]. However, at physiologic concentrations, the sole function of this peptide is to regulate iron homeostasis. The iron export transporter ferroportin, expressed on the basolateral membrane of intestinal cells and on the plasma membrane of macrophages, is the target for hepcidin [4,5]. Upon interaction with hepcidin, ferroportin undergoes proteosomal degradation, consequently resulting in decreased delivery of dietary iron from the intestinal cells into the blood and decreased release of iron from macrophages that originate from degradation of hemoglobin and other heme-containing proteins. Thus, elevated levels of hepcidin in the circulation cause systemic iron deficiency whereas decreased levels of hepcidin cause iron overload. The expression of hepcidin in the liver is under strict regulatory control; three proteins, namely, HFE (histocompatibility antigen associated with iron [Fe] regulation or high Fe), hemojuvelin (HJV or HFE2), and interleukin-6 (IL-6), have robust control of the transcription of *HAMP*, all facilitating hepcidin expression [1,2,4-9]. Inactivating mutations in HFE and HJV lead to decreased circulating levels of hepcidin, resulting in the genetic iron-overload disease, known as hereditary hemochromatosis [1,2]. The same is true with inactivating mutations in hepcidin [1,2].

Correspondence to: Vadivel Ganapathy, Department of Biochemistry and Molecular Biology, Cancer Center, 1410 Laney Walker Boulevard, Georgia Regents University, Augusta, GA, 30912; Phone: (706) 721-7652; FAX: (706) 721-9947; email: vganapat@gru.edu

HJV is a membrane-bound protein anchored to the lipid bilayer via glycosylphosphatidylinositol [10]. HJV also exists in a soluble form as a result of proteolytic cleavage by the enzyme furin [11]. When present in the membrane-bound form, HJV serves as a coreceptor for bone morphogenetic proteins, particularly BMP6, and induces hepcidin expression via phosphorylation of Smads 1/5/8 [12,13]. The soluble form of HJV traps BMPs by binding to them, and consequently blocks BMP signaling, phosphorylation of Smads, and transcription of *HAMP* [10,14]. IL-6 induces *HAMP* transcription through phosphorylation of STAT3 [15]; this activity is responsible for elevation of circulating levels of hepcidin during inflammation, causing inflammation-associated anemia [16]. The mechanism by which HFE induces *HAMP* expression remains unknown.

Iron is obligatory for normal function of the retina. Since excess iron can cause oxidative damage whereas iron deficiency would compromise retinal function, iron levels in the retina must be tightly regulated. Until recently, it was assumed that the retina is immune to changes in circulating levels of iron because of the presence of the blood–retinal barrier. However, recent studies have shown that retinal iron levels are drastically altered in diseases associated with disruption of systemic iron levels [17,18]. However, this is not because the retinal iron levels respond passively to circulating levels of iron but because almost all iron-regulatory proteins that are expressed in the liver and other tissues are also expressed in the retina. Importantly, evidence has emerged in recent years to indicate that the retina maintains significant autonomous control in iron homeostasis [17,18]. Various cell types within the retina actively participate in maintaining iron homeostasis. HFE is expressed exclusively in the RPE where the presence is restricted to the basolateral membrane [19]. HJV is expressed in all cell retinal cell types, and its expression in RPE is restricted to the apical membrane [20]. Hepcidin is expressed throughout the retina [21,22]. Dysregulation of retinal iron homeostasis in humans and mice resulting in increased accumulation of iron within the retinal tissue is associated with a phenotype resembling age-related macular degeneration [22-29].

More recently, a new regulator of systemic iron status has been discovered. The serine protease matriptase-2 (also known as TMPRSS6; transmembrane protease serine 6), has emerged as a critical regulator of iron homeostasis. Matriptase-2 is a membrane-bound enzyme that cleaves membrane-associated HJV and thus blocks the ability of HJV to induce hepcidin production [30,31]. The soluble form of HJV that is produced by furin-mediated cleavage is not a substrate for matriptase-2 [32]. Inactivating mutations in *TMPRSS6* lead to elevated levels of membrane-bound HJV, increased BMP signaling, and abnormally high levels of hepcidin [33,34]. The consequence of such mutations is systemic iron deficiency and the disease is called iron-refractory iron-deficiency anemia (IRIDA) [33,34]. Since we have shown recently that HJV is expressed robustly in all retinal cell types and plays an important role in retinal iron homeostasis [20], we asked whether the newly identified iron regulator matriptase-2 has any role in retinal iron status. No information is available in the literature on the expression or function of this enzyme in the retina. The purpose of the present study was to examine the expression of matriptase-2 in the retina and investigate the relevance to retinal iron homeostasis using the matriptase-2 knockout mouse (known as *mask* mouse because of the characteristic loss of hair in the body trunk but preservation of facial hair) [35]. In this mouse, matriptase-2 is synthesized as a truncated protein that has no catalytic activity due to the deletion of the entire serine protease domain located in the C-terminal domain [32,35].

METHODS

Reagents: Reagents were obtained from the following sources: reagent for RNA preparation (TRIzol; Invitrogen-Gibco, Grand Island, NY); Dulbecco's Modified Eagle Medium:Nutrient Mixture F-12 (DMEM/F12) culture medium (Invitrogen, Carlsbad, CA), RT–PCR kit (Applied Biosystems, Foster City, CA), *Taq* polymerase kit (TaKaRa, Tokyo, Japan), normal donkey serum (Jackson ImmunoResearch, West Grove, PA), and JB-4 solutions (Polysciences, Warrington, PA). The following antibodies were used: chicken anti-MCT1 (Alpha Diagnostic International, San Antonio, TX), goat anti-neogenin and rabbit anti-IL-6 (Santa Cruz Biotechnology, Santa Cruz, CA), rabbit anti-hepcidin (Abcam, Cambridge, MA), rabbit anti-Smad5 and rabbit anti-pSmad1/5/8 (Cell Signaling, Danvers, MA), rabbit anti-hemojuvelin (GenScript, Piscataway, NJ), mouse monoclonal anti-pSTAT3 (Cell Signaling), and rabbit anti-transferrin receptor 1 (Alpha Diagnostic International). Two different rabbit polyclonal antibodies specific for matriptase-2 (Abcam) were used: one (catalog # ab28287) targeted against the stem region of the protein, which is present in the truncated matriptase-2 expressed in the *Tmprss6*$^{msk/msk}$ mouse, and the other (catalog # ab42463) targeted against the C-terminal catalytic domain of the protein, which is absent in the truncated matriptase-2 expressed in the *Tmprss6*$^{msk/msk}$ mouse. Rabbit anti-H-ferritin and rabbit anti-L-ferritin antibodies were a generous gift from Dr. Paolo Arosio, University of Brescia, Brescia, Italy. Goat anti-chicken immunoglobulin G (IgG) coupled to Alexa Fluor 568, donkey anti-goat IgG coupled to Alexa Fluor 568, and

donkey anti-rabbit IgG coupled to Alexa Fluor 568, 555, and 488 were purchased from Molecular Probes (Carlsbad, CA).

Animals: Breeding pairs of *matriptase-2* heterozygous mice (*Tmprss6*^{msk}) on a C57BL/6 background were purchased from the Scripps Research Institute (La Jolla, CA). The homozygous knockout *mask* females (*Tmprss6*$^{msk/msk}$) are sterile because of the profound iron deficiency that cannot support pregnancy. Therefore, we generate the *mask* mice for our studies by crossing *mask* males with heterozygous females; even with this breeding scheme, the litter size is always small, indicating significant prenatal lethality. Genotyping was performed to identify wild-type, heterozygous (*Tmprss6*^{msk}), and homozygous (*Tmprss6*$^{msk/msk}$) mice in the litters. Age-matched wild-type and knockout (*Tmprss6*$^{msk/msk}$) mice were selected from the same litters for comparison studies. The knockout mice have a homozygous mutation in *matriptase-2* induced by *N*-ethyl-*N*-nitrosourea, which results in a truncated matriptase-2 with no proteolytic active site located at the C-terminal tail (matriptase-2 null) [35]. All procedures involving mice were approved by the Institutional Committee on Animal Use for Research and Education at the Georgia Regents University and were performed in accordance with the ARVO Statement for the Use of Animals in Ophthalmic and Vision Research.

Preparation of eye sections and immunofluorescence analysis: Mice were killed by carbon dioxide asphyxiation followed immediately by cervical dislocation. For studies using frozen sections, eyes were enucleated and oriented in Tissue-Tek O.C.T. compound so that the 10-µm-thick sections included the full length of the retina approximately along the horizontal meridian, passing through the ora serrata and the optic nerve in the temporal and nasal hemispheres. After rapid freezing in liquid nitrogen, the cryosections were prepared and mounted on slides (Superfrost; Fisher Scientific). They were stained with hematoxylin and eosin (H&E) to examine morphology. Additional cryosections were used for immunohistochemical studies.

Cryosections of mouse eyes were fixed in 4% (v/v) paraformaldehyde for 10 min, washed with 0.01 M Dulbecco's PBS (1X; 1.5 mM KH_2PO_4, 8.1 mM Na_2HPO_4, 137 mM NaCl, 2.7 mM KCl)/0.1% Triton X-100 (pH 7.4), and blocked with 4% normal donkey serum for 1 h. Sections were then incubated overnight at 4 °C with one or more of the following primary antibodies: chicken anti-MCT1 (1:1,000), goat anti-neogenin (1:100), rabbit anti-matriptase 2 (1:50), rabbit anti-H-ferritin (1:2,000), rabbit anti-L-ferritin (1:2,000), rabbit anti-hemojuvelin (1:100), rabbit anti-hepcidin (1:100), rabbit anti-Smad5 (1:50), rabbit anti-pSmad1/5/8 (1:50), and rabbit anti-IL-6 (1:200). Negative control sections were treated identically, but in the absence of the primary antibody. Sections were rinsed and incubated for 1 h with the corresponding secondary antibody, either independently or together as needed, at a dilution of 1:1,000. Coverslips were mounted after staining with Hoechst nuclear stain, and sections were examined with a fluorescence microscope (Leica DM5500B, Leica Microsystems, Buffalo Grove, IL) or laser-scanning confocal microscopy (Carl Zeiss Meditec).

JB-4 plastic sections and morphometric analysis: Eyes were enucleated and fixed for 1 h at room temperature (22 °C) in 2% (w/v) paraformaldehyde/0.2% glutaraldehyde in 0.1 M sodium cacodylate/HCl buffer (pH 7.4) in sucrose and post-fixed for 1 h with 1% tannic acid in 0.1 M sodium cacodylate buffer. Tissues were dehydrated using a graded series of ethanol solutions and infiltrated overnight in 1.25% benzoyl peroxide using the JB-4 embedding kit. The next day, the eyecups were oriented and embedded in plastic as recommended in the embedding kit. Sections, 2-µm thick, were cut and used for histological analysis after H&E staining.

H&E-stained sections of retinas from 5-month-old *Tmprss6*$^{msk/msk}$ mice along with age-matched wild-type mice were used for systematic morphometric analysis with a fluorescence microscope (Leica DM5500B, equipped with a DFC450 camera and the LAS AF program). Measurements included the thicknesses of the total retina, RPE, inner plexiform layer (IPL), inner nuclear layer (INL), outer plexiform layer (OPL), outer nuclear layer (ONL), and the photoreceptor inner/outer segments. The number of cell bodies in the ganglion cell layer (GCL) was quantified by counting cells from the temporal ora serrata to the nasal ora serrata, and the data are expressed as number of cells per 100-µm length of retina. Three measurements were made on each side (temporal and nasal) of the optic nerve at 200- to 300-µm intervals, resulting in six measurements per eye. Two measurements on either side of the optic nerve were taken as the central retina, and the remaining four measurements from that eye were considered the peripheral retina. Both eyes were analyzed in each mouse. Statistical analysis was performed with the Student paired *t* test (wild-type versus knockout); $p<0.05$ was taken as significant.

Primary cultures of retinal pigment epithelium, Müller cells, and ganglion cells from mouse retinas: Cultures of RPE, Müller, and ganglion cells from mouse retinas were established as described previously [36-38]. Total RNA was isolated from these primary cultures for analyzing mRNA levels for matriptase-2, hemojuvelin, and neogenin.

RT–PCR: : RNA was isolated from the wild-type and *Tmprss6*$^{msk/msk}$ mice by TRIzol extraction, and RT–PCR was performed using the GeneAmp RT–PCR kit. PCR primers

Table 1. Sequences of RT-PCR primers used in the present study.

Gene	Species	Primer sequence (5'-3')	Product size (bp)
HFE	Mouse	F:GGCTTCTGGAGATATGGTTAT	142
		R:GACTCCACTGATGATTCCGATA	
Hepcidin	Mouse	F:GCACCACCTATCTCCATCAACAGA	188
		R:GGTCAGGATGTGGCTCTAGGCTAT	
Hemojuvelin	Mouse	F:GGCTGAGGTGGACAATCTTC	551
		R:GAACAAAGAGGGCCGAAAG	
TfR1	Mouse	F:GCCCAAGTATTCTCAGATATGAT	633
		R:TAGAAGTAGCACGGAAGTAGTCTC	
Matriptase-2	Mouse	F:CCCTCTCTGGACTACGGCTTGGC	842
		R:CGGCTCACCTTGAAGGACAC	
Neogenin	Mouse	F:TCGAACATTCACTCCGTTTTA	621
		R:CGCATCAGAAATACCAAGTCTAC	

were designed based on the sequence information available in GenBank for mouse cDNAs. The primer sequences are given in Table 1. PCR was performed using a commercially available Taq polymerase kit. The sizes of the PCR amplicons were as follows: matriptase-2, 842 bp; neogenin, 621 bp; hemojuvelin, 551 bp; HFE, 142 bp; hepcidin, 188 bp; TfR1, 633 bp.

The following primers were used to quantify ID1 mRNA in the mouse retina with real-time PCR: forward primer 5′-CGA CTA CAT CAG GGA CCT GCA-3′ and reverse primer 5′-GAA CAC ATG CCC CCT CGG-3′. For HFE, hepcidin, hemojuvelin, and TfR1, the same primer pairs described for RT–PCR were also used for real-time PCR. Real-time amplifications, using SYBR Green detection chemistry (Applied Biosystems), were run in triplicate on 96-well reaction plates.

Data analysis: All experiments were repeated three to five times with independent cell or tissue preparations and samples run in duplicate. Data are presented as mean±standard error of the mean (SEM). Statistical significance was determined with the Student t test and one-way ANOVA with Tukey-Kramer's post-hoc tests for comparisons between two groups or multiple groups, respectively. Differences were considered statistically significant at $p<0.05$.

RESULTS

Expression of matriptase-2 in the mouse retina and its colocalization with hemojuvelin in the apical membrane of retinal pigment epithelium: We first used RT–PCR to examine the expression of matriptase-2 and its substrate hemojuvelin in the mouse retina and in primary cultures of mouse RPE, Müller cells, and ganglion cells. Matriptase-2 mRNA was present in the neural retina as well as in RPE/eyecup and was detected in primary cultures of RPE, Müller cells, and ganglion cells (Figure 1A). Similarly, hemojuvelin was also expressed in the neural retina, RPE/eyecup, and primary cultures of all three retinal cell types examined (RPE, Müller cells, and ganglion cells). Neogenin is a receptor for the repulsive guidance molecules (RGMs), and hemojuvelin, also called RGMc, is a member of this group. Recently, neogenin has been shown to be a regulator of hepcidin expression in the liver; deletion of neogenin leads to reduced BMP signaling, decreased hepcidin expression, and enhanced accumulation of iron in the liver [39]. Neogenin is required for the control of hepcidin expression by hemojuvelin; it interacts with matriptase-2 and hemojuvelin in a ternary complex and facilitates the cleavage of membrane-bound hemojuvelin by matriptase-2 [39]. Therefore, we monitored the expression of neogenin in the mouse retina with RT–PCR and found the expression pattern of neogenin mRNA to be as ubiquitous as that of matriptase-2 mRNA and hemojuvelin mRNA (Figure 1A). Immunofluorescence analysis of matriptase-2 protein paralleled its mRNA expression pattern (Figure 1B). The protein was detected in ganglion cells, Müller cells, and RPE. It was also present in various other neuronal cells, including the photoreceptor cells. We then focused on RPE, a polarized cell with its apical membrane facing the subretinal space and the basolateral membrane facing the choroidal circulation, for the expression of matriptase-2. Since we have previously shown that hemojuvelin is expressed only on the apical membrane of RPE [20], it was important to know if matriptase-2 and

its proteolytic substrate hemojuvelin are colocalized in the same membrane. It was indeed the case (Figure 1C). The apical membrane localization of matriptase-2 was further confirmed by its colocalization with MCT1, a marker for RPE apical membrane. In contrast, there was no evidence of colocalization for matriptase-2 and *HFE*, an iron-regulatory protein that is present only in the basolateral membrane of RPE. Neogenin was also found in the RPE apical membrane (Figure 1C).

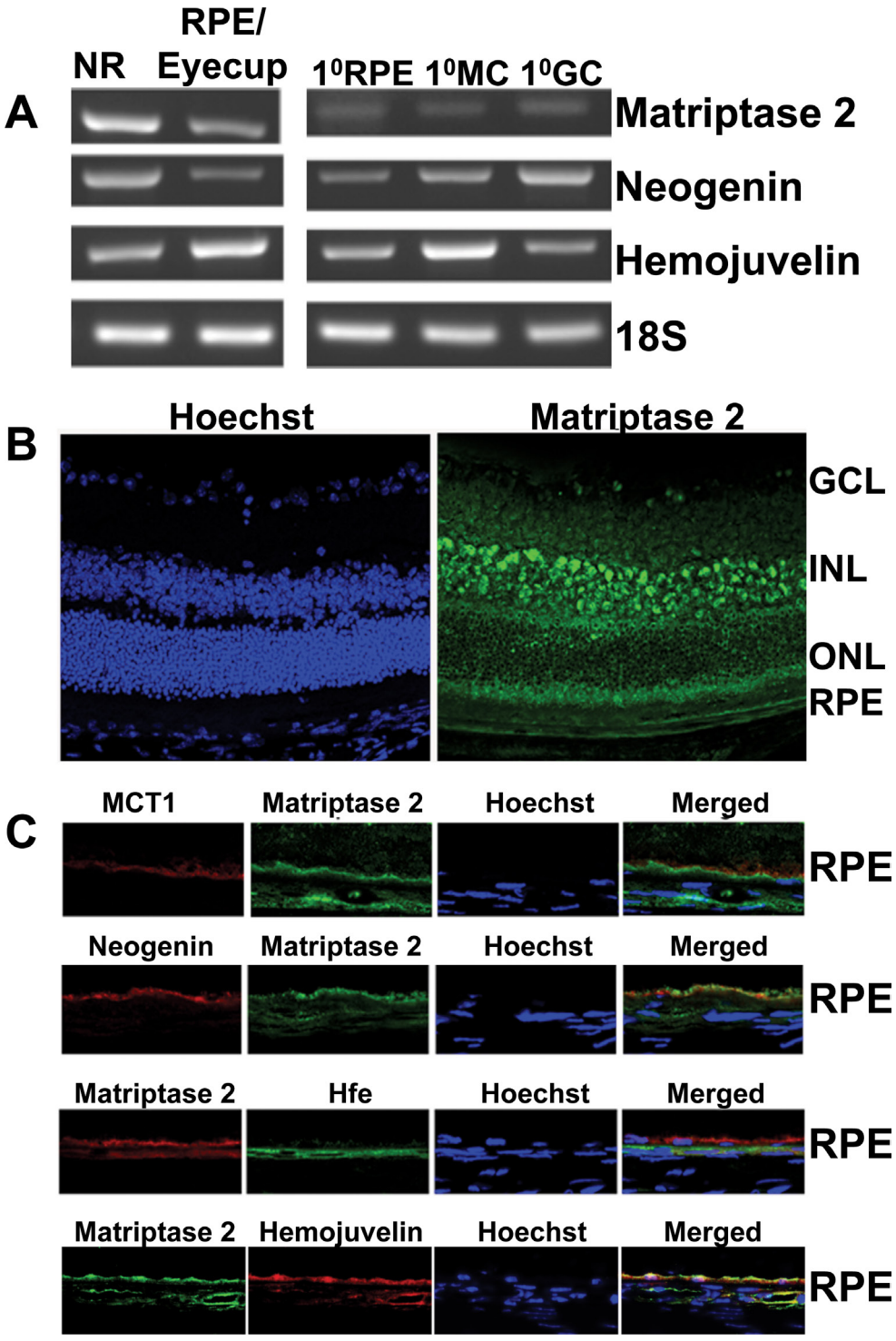

Figure 1. Expression of matriptase-2 in the mouse retina. **A**: RT–PCR analysis of mRNAs for matriptase-2, neogenin, and hemojuvelin in the neural retina (NR) and the RPE/eyecup and in primary cultures of RPE (1°RPE), Müller (1°MC), and ganglion (1°GC) cells isolated from mouse eyes. 18S was used as an internal control. RT–PCR was repeated with RNA preparations from three different mice, and the results were similar. **B**: Immunofluorescence localization of matriptase-2 protein in the mouse retina: left-hand panel, nuclear specific Hoechst staining; right-hand panel, pattern of matriptase-2 expression. GCL, ganglion cell layer; INL, inner nuclear layer; ONL, outer nuclear layer; RPE, retinal pigment epithelium. **C**: Polarized expression of matriptase-2 in RPE investigated by comparing its expression pattern with that of monocarboxylate transporter 1 (MCT1; a marker of RPE apical membrane) and Hfe (a marker for basolateral membrane). In addition, the relationship between the expression pattern in the RPE of matriptase-2 with that of neogenin (a protein that interacts with hemojuvelin) and hemojuvelin (the substrate for matriptase-2) was also studied. The immunocomplexes were detected with appropriate secondary antibodies conjugated to either Alexa Fluor 568 (red) or Alexa Fluor 488 (green). Immunofluorescence localization studies were repeated with retinal sections prepared from two different mice.

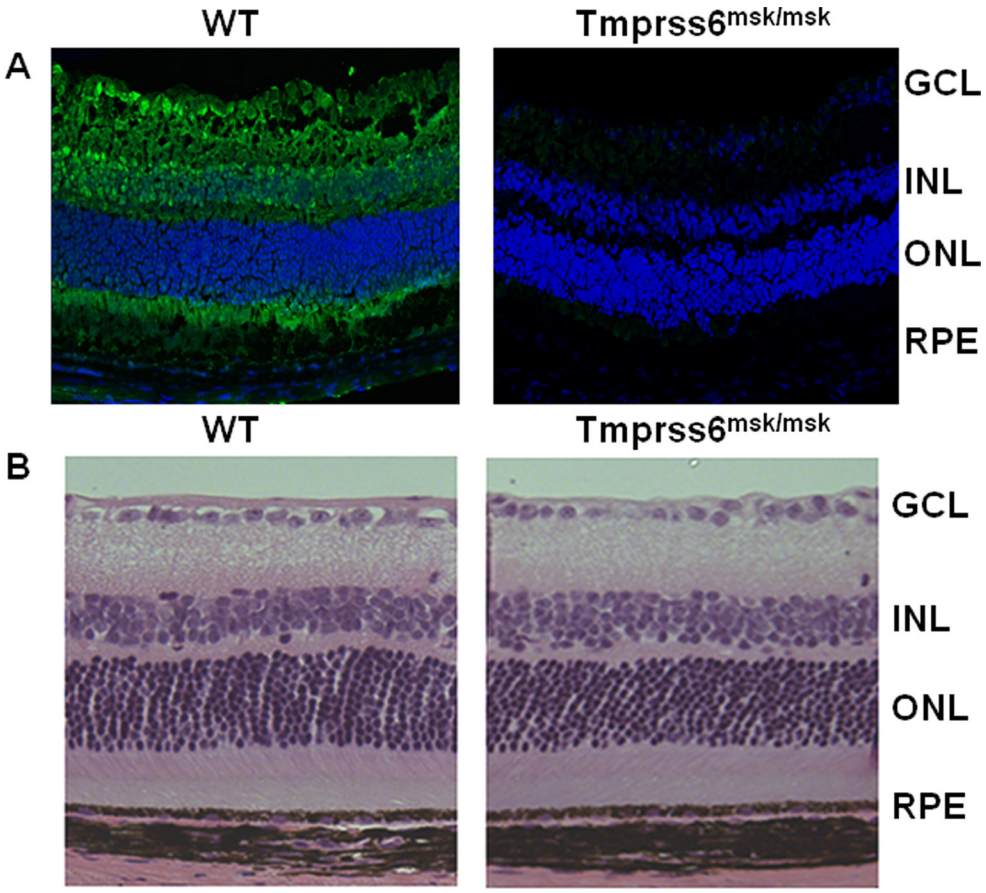

Figure 2. Specificity of matriptase-2 staining in retina and retinal morphology in wild-type and *Tmprss6*$^{msk/msk}$ mice. **A**: The expression pattern of matriptase-2 was analyzed in retinal sections prepared from wild-type mice and *Tmprss6*$^{msk/msk}$ mice using an antibody specific for the C-terminal tail of the matriptase-2 protein. The *Tmprss6*$^{msk/msk}$ mouse expresses a truncated matriptase-2 that lacks the C-terminal tail. The experiment was repeated twice with retinal sections from different wild-type mice and *Tmprss6*$^{msk/msk}$ mice. **B**: Retinal morphology as assessed with hematoxylin and eosin staining of retinal sections from wild-type and *Tmprss6*$^{msk/msk}$ mice. Eyes from 5-month-old wild-type and *Tmprss6*$^{msk/msk}$ mice were enucleated, fixed, and embedded in JB-4. Sections were cut at 2-µm thickness and examined with light microscopy. The morphology was examined individually with retinal sections prepared from four wild-type mice and four *Tmprss6*$^{msk/msk}$ mice, and the results were similar.

Specificity of matriptase-2 immunostaining in the retina and morphology of retina in matriptase-2-knockout (Tmprss6$^{msk/msk}$) mice: To determine the specificity of the matriptase-2 staining in the retina described in Figure 1B, we wanted to compare the immunostaining between the retinal sections prepared from wild-type mice and matriptase-2 knockout (*Tmprss6*$^{msk/msk}$) mice. However, the antibody we used initially to generate the data in Figure 1B was not suitable for this purpose. This particular antibody was raised against a peptide sequence located in the stem region of matriptase-2; but the *mask* mice (*Tmprss6*$^{msk/msk}$) express a truncated matriptase-2 protein that still contains the stem region [35]. Therefore, we used another antibody that was targeted against the protease catalytic site located in the C-terminal domain of the protein; this region is absent in the truncated protein generated in the *mask* mouse. With this antibody, we compared the matriptase-2 immunostaining in retinal sections between wild-type mice and *Tmprss6*$^{msk/msk}$ mice. Again, the expression of matriptase-2 was evident in all layers of the retina when examined with the retinal sections from wild-type mice, but the staining was completely absent in retinal sections from the knockout mice when processed under identical conditions (Figure 2A). These data confirm the specificity of the matriptase-2 antibody and thus the specificity of the immunostaining observed in the wild-type mouse retina.

We have shown previously that deletion of *HFE* and *HJV* in mice leads to excessive iron accumulation in the retina and iron-induced oxidative stress, resulting in significant retinal degeneration [27,29]. Deletion of matriptase-2 in mice causes systemic iron deficiency [35], but the retina has not been evaluated in these mice. Therefore, we examined the retinal morphology in matriptase-2-knockout mice. When examined with 3-month-old or 5-month-old mice, the gross morphology of the retina was not different between the *Tmprss6*$^{msk/msk}$ mice and the age-matched wild-type mice (Figure 2B). However, an in-depth morphometric analysis revealed small, but significant, differences in specific parameters in 5-month-old wild-type and *Tmprss6*$^{msk/msk}$ mice (Figure 3). This included an increase in the thickness of the whole retina as well as various individual nuclear and cell layers in the

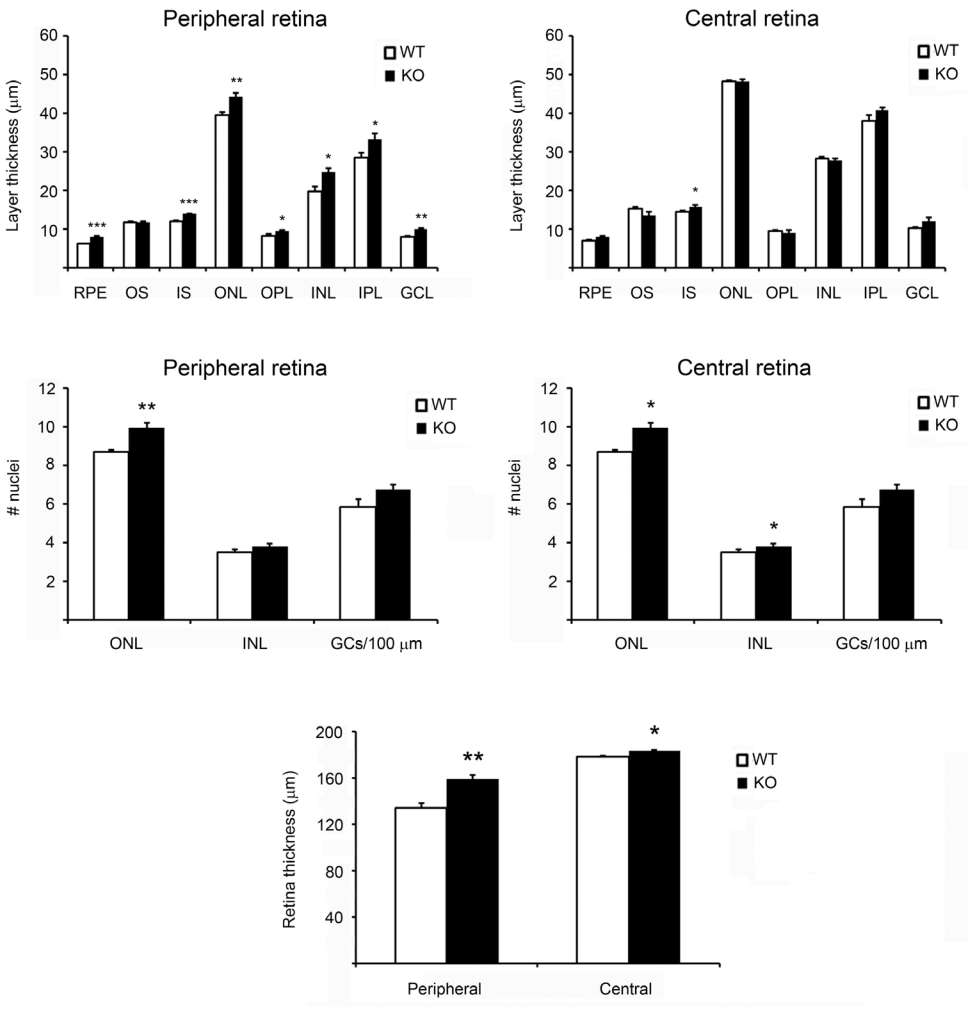

Figure 3. Morphometric analysis of peripheral and central retinas from wild-type mice and *Tmprss6*$^{mas/msk}$ mice. The parameters measured included the thickness of various cell layers, the number of cell nuclei in various cell layers, and the thickness of the entire retina. Measurements were made in the central retina as well as in the peripheral retina. * p<0.05; ** p<0.01; *** p<0.001. RPE, retinal pigment epithelium; OS, outer segment of photoreceptors; IS, inner segment of photoreceptors; ONL, outer nuclear layer; OPL, outer plexiform layer; INL, inner nuclear layer; IPL, inner plexiform layer; GCL, ganglion cell layer. Results are from the analysis of retinal sections from three wild-type mice and three *Tmprss6*$^{msk/msk}$ mice.

Tmprss6$^{msk/msk}$ mouse. This difference was more prominent in the peripheral retina than in the central retina. Such changes, however, were not detectable in 3-month-old *Tmprss6*$^{msk/msk}$ mice (data not shown). These results suggest that the changes in retinal morphology in the *Tmprss6*$^{msk/msk}$ mouse represent an age-dependent phenomenon. Since the *Tmprss6*$^{msk/msk}$ mice die prematurely due to severe iron deficiency, we were not able to analyze the retinal morphology in these mice beyond 5 months of age.

Evidence of iron deficiency in the mask mouse retina: Systemic iron deficiency has been demonstrated in *Tmprss6*$^{msk/msk}$ mice [35]. Here we examined the iron status in the retina in the *Tmprss6*$^{msk/msk}$ mouse. We used the expression levels of H-ferritin and L-ferritin to monitor the iron status. Ferritin is an intracellular iron-storage protein, and its levels go up in iron overload but go down in iron deficiency. With immunofluorescence analysis, we found the levels of the heavy (H) and light (L) chains of ferritin were lower in the *Tmprss6*$^{msk/msk}$ mouse (5-month-old) retina than in the age-matched wild-type mouse retina (Figure 4A). RT–PCR analysis revealed marked upregulation in the expression of the iron-regulatory genes *HJV*, *HAMP* (the gene coding for the iron-regulatory hormone hepcidin), and *TfR1* (the gene coding for the transferrin receptor 1 that mediates iron uptake in most tissues; Figure 4B). Quantitative PCR confirmed the upregulation of these three genes. The steady-state levels of mRNAs for HJV, hepcidin, and transferrin receptor 1 increased in the knockout mouse retina sixfold, threefold, and fivefold, respectively. The expression of HFE was reduced in the knockout mouse retina slightly. The increased expression of TfR1 is a strong indicator of iron deficiency. We confirmed this finding by monitoring the TfR1 protein levels with immunofluorescence (Figure 5). The upregulation of HJV and hepcidin at the mRNA level was also confirmed at the protein level with immunofluorescence (Figure 6A). Since hepcidin is the hormone that most other iron-regulatory

proteins converge upon to elicit their control over iron homeostasis, we examined the changes in the mRNA levels of hepcidin specifically in the neural retina versus the RPE/eyecup (Figure 6B). Interestingly, the upregulation of *HAMP* expression observed in the *mask* mouse retina was confined to the neural retina. There was no change in hepcidin mRNA levels in the RPE/eyecup between wild-type mice and the *Tmprss6*$^{msk/msk}$ mice. These studies clearly demonstrate that the defective function of matriptase-2 causes iron deficiency in the retina.

Molecular mechanism of hepcidin upregulation in the mask mouse retina: Hemojuvelin induces the expression of the *HAMP* through BMP signaling [12-14]. It has also been shown that BMP signaling is upregulated in the *Tmprss6*$^{msk/msk}$ mouse liver, which links the increased expression of hemojuvelin and the increased expression of hepcidin [35]. Based on these findings in the *Tmprss6*$^{msk/msk}$ mouse liver, we predicted a similar mechanism for the upregulation of hepcidin in *Tmprss6*$^{msk/msk}$ mouse retina. To test the validity of this prediction, we analyzed BMP signaling in the retinas from the 5-month-old wild-type and *Tmprss6*$^{msk/msk}$ mice. Contrary to our prediction, BMP signaling was decreased in the *Tmprss6*$^{msk/msk}$ mouse retinas compared to the wild-type mouse retinas as evidenced from the decreased phosphorylation of Smad1/5/8 with no difference in total Smad5 protein levels (Figure 7A). The decreased BMP signaling in the *mask* mouse retinas was confirmed by the downregulation of the expression of *ID1*, a target for BMP signaling (Figure 7B). These data demonstrate that hepcidin expression in the *Tmprss6*$^{msk/msk}$ mouse retina is upregulated despite the decreased BMP signaling, suggesting some other mechanism. The proinflammatory cytokine IL-6 is a potent inducer of

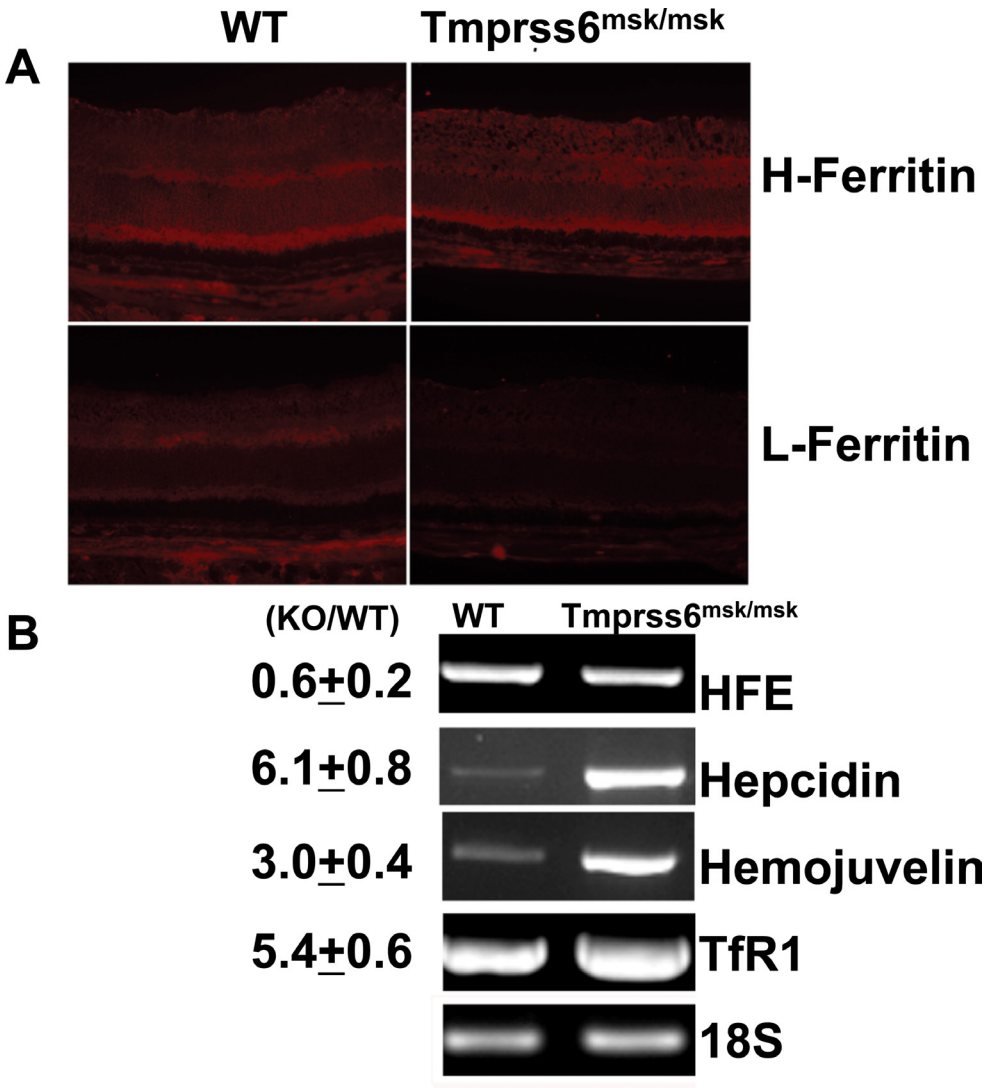

Figure 4. Expression of H-ferritin and L-ferritin and reverse transcription-polymerase chain reaction (RT-PCR)/quantitative PCR (qPCR) analysis of mRNA levels for various iron-regulatory genes in wild-type and *Tmprss6*$^{msk/msk}$ mouse retinas. **A**: Expression of H-ferritin and L-ferritin was examined with immunofluorescence in 4-week-old wild-type and *Tmprss6*$^{msk/msk}$ mouse retinal cryosections. Results are representative of the experiments performed with two wild-type mice and two *Tmprss6*$^{msk/msk}$ mice; two different retinal sections were examined for each mouse. **B**: RT–PCR and qPCR analyses of mRNA levels of various iron-regulatory genes in wild-type and *Tmprss6*$^{msk/msk}$ mouse retinas (RPE/eyecup plus neural retina). 18S was used as an internal control. The values (mean±SE), obtained with RNA preparations from the retinas of three wild-type mice and three *Tmprss6*$^{msk/msk}$ mice, represent fold changes in mRNA levels in the knockout mouse retina compared to the wild-type retina (KO/WT) as assessed with qPCR.

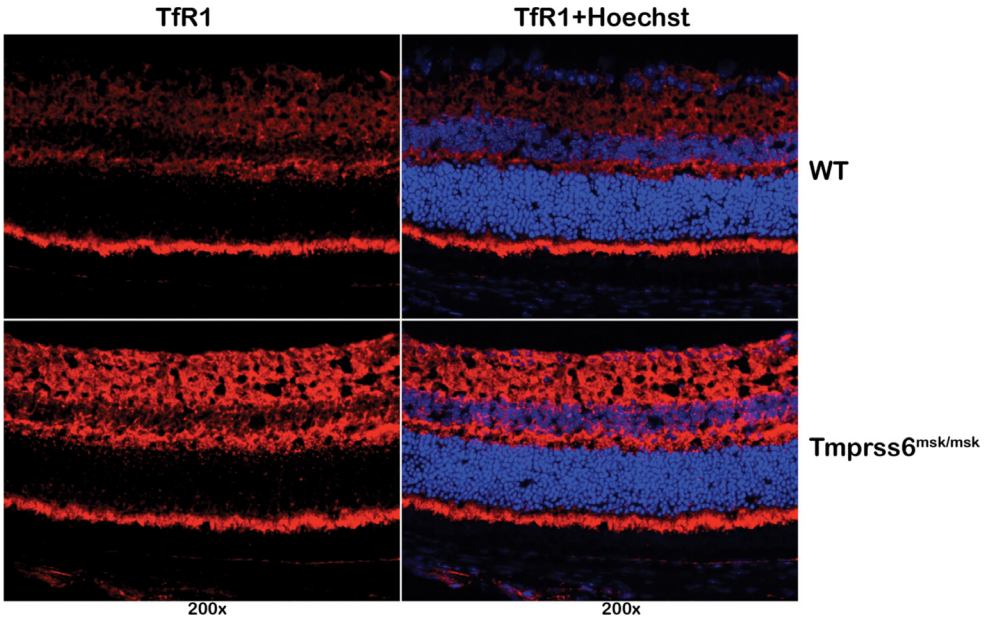

Figure 5. Expression of transferrin receptor 1 in wild-type and *Tmprss6*$^{msk/msk}$ mouse retinas as assessed with immunofluorescence. Hoechst was used as the nuclear stain. Results shown are representative of the experiments performed with retinal sections from three wild-type mice and three *Tmprss6*$^{msk/msk}$ mice.

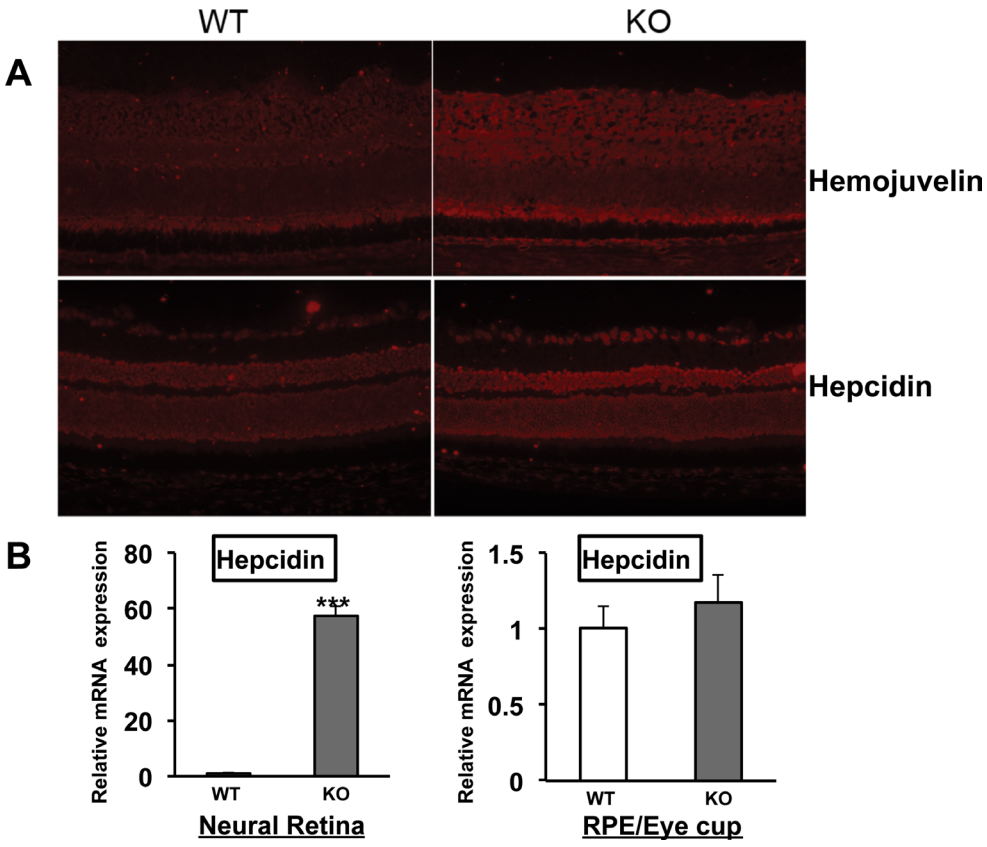

Figure 6. Expression of hemojuvelin and hepcidin in wild-type and *Tmprss6*$^{msk/msk}$ mouse retinas. **A**: Immunofluorescent staining of retinal cryosections from 4-week-old wild-type (WT) and *Tmprss6*$^{msk/msk}$ (KO) mice was performed for hemojuvelin and hepcidin. The experiment was repeated with two mice (four retinas) for each genotype. **B**: The neural retina and the RPE/ eyecup were isolated from the wild-type and *Tmprss6*$^{msk/msk}$ mice, and the RNA samples isolated from these preparations were used for qPCR to assess hepcidin mRNA levels. Data represent the results from three independent RNA preparations (three wild-type mice and three *Tmprss6*$^{msk/msk}$ mice). *** $p<0.001$.

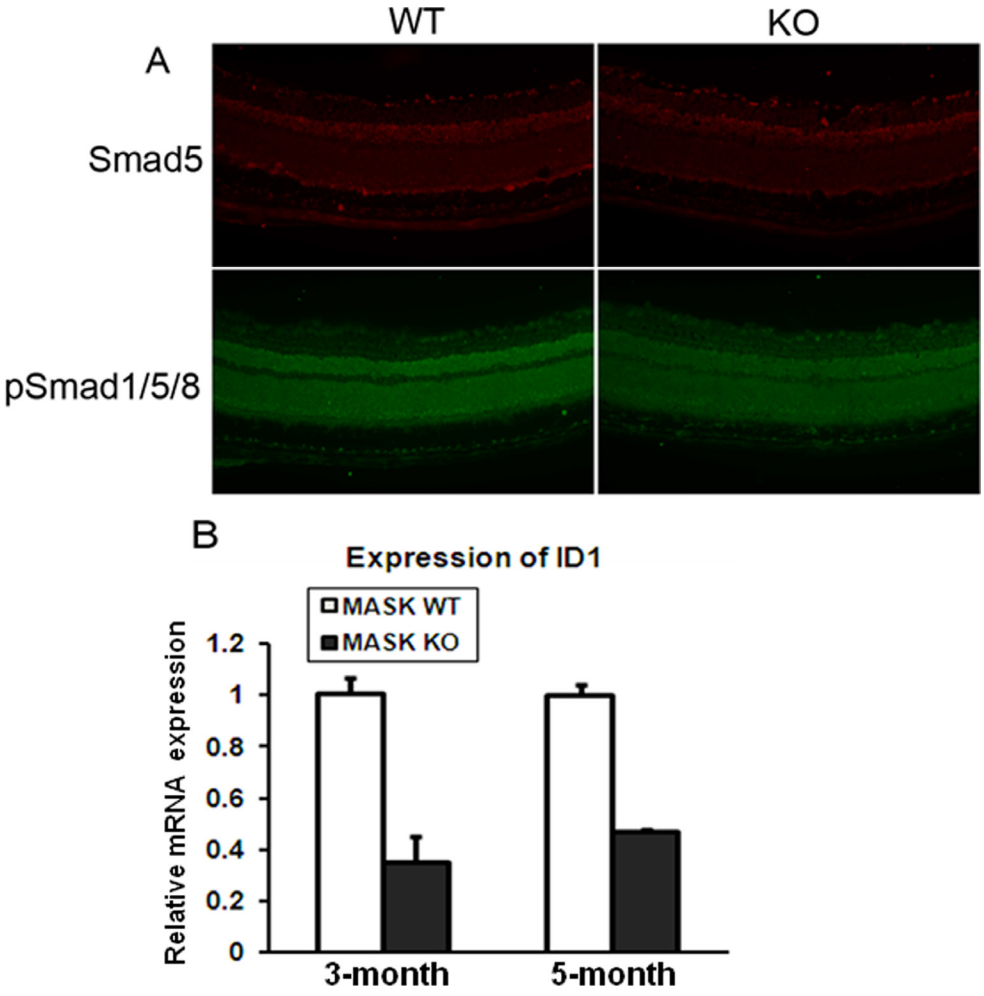

Figure 7. Bone morphogenetic protein signaling in wild-type and *Tmprss6*$^{msk/msk}$ mouse retinas. **A**: Retinal cryosections from wild-type (WT) and *Tmprss6*$^{msk/msk}$ (KO) mice were subjected to immunofluorescence to detect Smad5 and phosphorylated Smad1, Smad5, and Smad8 (pSmad1/5/8). The experiment was repeated with two mice (four retinas) for each genotype. **B**: qPCR analysis was performed to quantify ID1 (inhibitor of differentiation-1) mRNA levels in 3-month-old and 5-month-old wild-type (WT) and *Tmprss6*$^{msk/msk}$ (KO) mouse retinas. Data are presented as the fold change in the KO retina relative to the WT retina. Data represent the results from three independent RNA preparations (three wild-type mice and three *Tmprss6*$^{msk/msk}$ mice). ***, p<0.001.

hepcidin expression [15]; therefore, we compared IL-6 expression in the retina between the wild-type and *Tmprss6*$^{msk/msk}$ mice. We found significant upregulation of IL-6 expression at the protein level (immunofluorescence; Figure 8A) and at the mRNA level (qPCR; Figure 8B). We also examined the changes in IL-6 signaling by monitoring the phosphoform of the transcription factor STAT3 by immunofluorescence. We found an increase in the levels of the phosphorylated form of STAT3 in the knockout mouse retinas compared to the wild-type mouse retinas (Figure 8C). These data show that the upregulation of hepcidin expression observed in the *Tmprss6*$^{msk/msk}$ mouse retina occurs not through BMP but most likely through IL-6.

DISCUSSION

In the present study, we report for the first time on the expression of matriptase-2 in the retina. The protein is expressed widely in the retina, with evidence of expression seen in the RPE, Müller cells, and ganglion cells. We recently reported that hemojuvelin, a substrate of matriptase-2, is expressed in the retina and that mice lacking hemojuvelin develop iron overload and retinal degeneration [20,29]. Matriptase-2 along with neogenin is known to cleave GPI-anchored HJV into a soluble form and thus block the ability of HJV to induce hepcidin production [30,31]. Thus, we wanted to understand the role of matriptase-2 in hemojuvelin-mediated retinal iron homeostasis. We found that in the RPE, the expression of matriptase-2 is restricted to the apical membrane that faces the neural retina. The specific colocalization of matriptase-2 in the apical membrane of the RPE along with hemojuvelin and neogenin is particularly exciting, given that all these three proteins interact together to regulate hepcidin expression [39]. The RPE is involved in the handling of iron arising from the continuous phagocytosis of outer rod segments. Thus, the RPE must have mechanisms to export iron to protect against the risk of excessive iron accumulation and consequent oxidative stress and tissue damage. The same is true also for heme, and RPE expresses two different heme

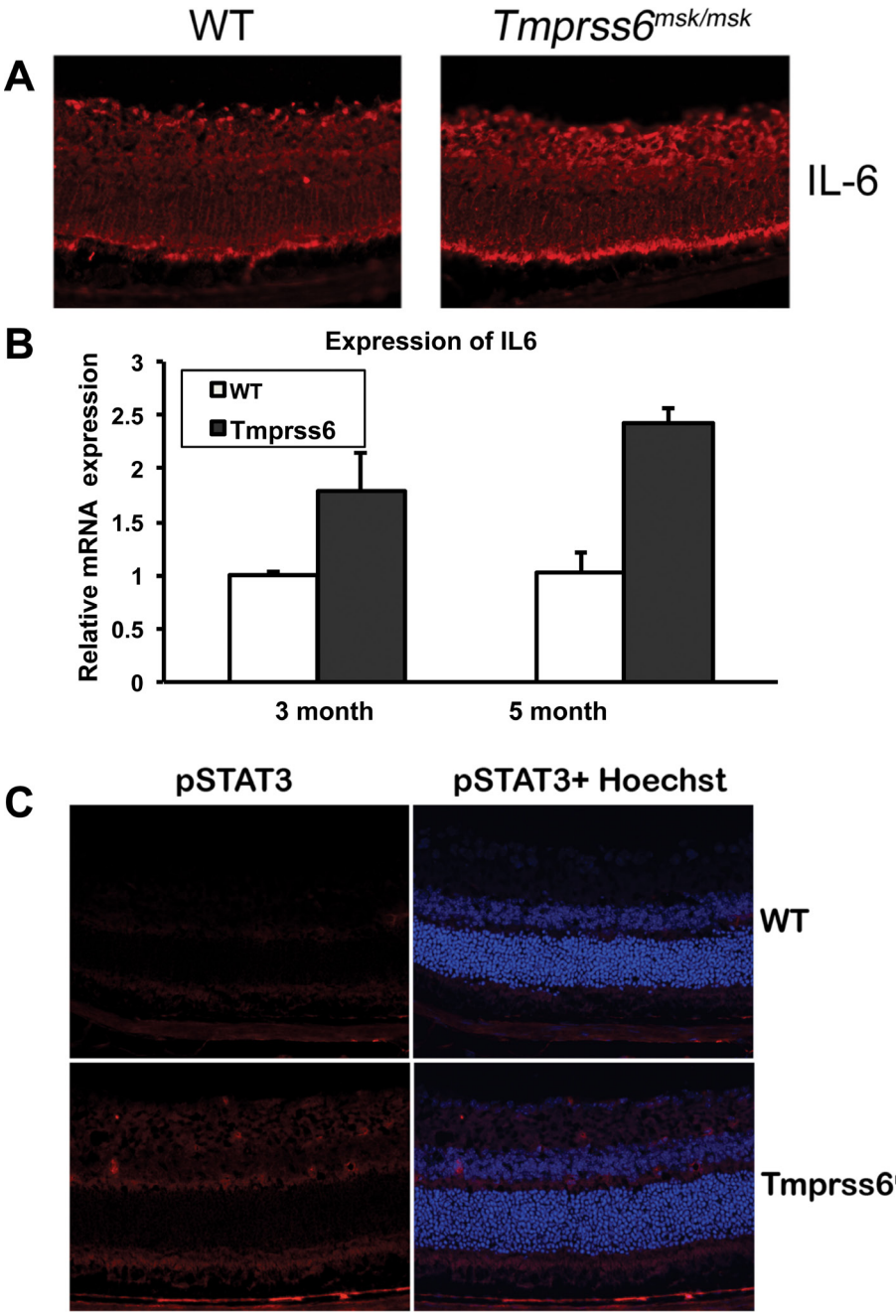

Figure 8. Interleukin-6 signaling in wild-type and *Tmprss6*$^{msk/msk}$ mouse retinas. **A**: Immunofluorescent analysis of interleukin-6 (IL-6) expression in wild-type (WT) and *Tmprss6*$^{msk/msk}$ mouse retinas using cryosections. The experiment was repeated with two mice (four retinas) for each genotype. **B**: qPCR analysis of IL-6 mRNA levels in 3-month-old and 5-month-old WT and *Tmprss6*$^{msk/msk}$ mouse retinas. Data are presented as the fold change in the *Tmprss6*$^{msk/msk}$ retina relative to the WT retina. Data represent the results from four independent RNA preparations (four wild-type mice and four *Tmprss6*$^{msk/msk}$ mice). *, $p<0.05$; ***, $p<0.001$. **C**: Immunofluorescent analysis of the expression of the phosphorylated form of STAT3 (pSTAT3) in wild-type (WT) and *Tmprss6*$^{msk/msk}$ mouse retinas using cryosections. The experiment was repeated with two mice (four retinas) for each genotype.

transporters in a polarized manner [40]. Iron export in other cell types is mediated almost exclusively by ferroportin, and the expression of this transporter has been reported in the RPE [22]. In our previous studies, we have demonstrated that hepcidin, which regulates ferroportin, is also expressed in the RPE [21]. We have also shown that the expression of hepcidin in the RPE is controlled by HFE and HJV during iron overload [27,29]. Hepcidin expression is also regulated during inflammation independent of HFE and HJV [21]. Thus, matriptase-2, neogenin, and hemojuvelin together may play a vital role in regulating the retinal iron homeostasis by regulating local production of hepcidin within the retina by the RPE and other retinal cell types.

In humans, matriptase-2 mRNA is detected almost exclusively in the liver [41]; in contrast, the expression is much more widespread in the mouse, with expression detectable not only in liver but also in other tissues such as the kidney and the uterus [42]. However, none of the reported

studies has examined the retina for matriptase-2 expression. The present study provides the first evidence for the expression of this important iron-regulatory protein in the retina. This finding strengthens the currently emerging view that the retina is equipped with all the mechanisms necessary for local control of iron homeostasis independent of systemic iron status. The present study showing the widespread expression of matriptase-2 in the retinal cells prompted us to examine the retina in matriptase-2 knockout mice. For this purpose, we used *Tmprss6*$^{msk/msk}$ mice, lacking a functional matriptase-2 protein, that has been reported to have elevated levels of membrane-bound HJV, increased BMP signaling in the liver, and abnormally high levels of hepcidin resulting in systemic iron deficiency [35]; however, the retina has not been examined in this mouse. In line with what was expected, we found that the *Tmprss6*$^{msk/msk}$ mice had iron deficiency in the retina marked by a decrease in H-ferritin and L-ferritin levels and drastic upregulation of hepcidin expression. Interestingly, despite the convincing evidence for iron deficiency within the retina in *Tmprss6*$^{msk/msk}$ mouse, there are no profound changes in retinal morphology and architecture. It is possible that iron deficiency in this mouse model is not severe enough to cause significant alterations in retinal morphology. Alternatively, the retinal changes that occur in response to iron deficiency might be an age-dependent phenomenon; since *Tmprss6*$^{msk/msk}$ mice succumb to death at an early age due to systemic iron deficiency, retinal changes promoted by iron deficiency may not become noticeable at such a young age. We noticed a small, but significant, increase in the thickness of various cell layers in the knockout mouse retina, but how iron deficiency causes these changes remains to be determined.

Inactivating mutations in matriptase-2 lead to iron-deficiency anemia that does not respond well to iron therapy because of the inability to decrease hepcidin production in the liver during iron deficiency [43]. Iron-deficient animals have enhanced expression of matriptase-2 in the liver, suggesting that downregulation of hepcidin expression in response to acute iron deficiency is mediated by an increase in matriptase-2 protein levels [44]. Matriptase-*2* regulates hepcidin expression in the liver through the suppression of BMP/Smad signaling by cleaving the BMP coreceptor HJV [30,31,45]. Livers from mice deficient in matriptase-2 have decreased iron stores and markedly increased mRNA for *ID1*, a target gene of BMP6 signaling [46]. Loss of BMP6 decreases hepcidin levels, increases hepatic iron, and, importantly, rectifies the abnormalities in matriptase-2 mutant mice [47]. Unlike in the liver, the BMP/Smad signaling was downregulated in the *Tmprss6*$^{msk/msk}$ mouse retina as evidenced from decreased *ID1* expression, a downstream target of BMP signaling. However, *hepcidin*, another target gene of BMP signaling, was upregulated many-fold in the *Tmprss6*$^{msk/msk}$ mouse retina, indicating alternative mechanisms for hepcidin upregulation independent of BMP signaling. Interestingly, earlier studies using double knockouts of matriptase-2 with either HFE or HJV have shown that hepatic hepcidin upregulation in *Tmprss6*$^{msk/msk}$ mice occurs irrespective of the presence or absence of HFE or HJV [48,49]. All these studies show that hepcidin can be upregulated in *Tmprss6*$^{msk/msk}$ mice independent of HFE and HJV; however, future studies should be aimed at understanding the reason for downregulation of BMP signaling in the retina opposite of the effect reported in the liver of *Tmprss6*$^{msk/msk}$ mice.

Hepcidin upregulation occurs either by BMP signaling or through inflammation mediated by IL-6 [50,51]. The elevated IL-6 expression coupled with decreased BMP signaling in the *Tmprss6*$^{msk/msk}$ mouse retina shows that the upregulation of retinal hepcidin expression in this mouse model is due to the proinflammatory cytokine IL-6 and not due to BMP. IL-6 influences gene expression through its cell-surface receptor, which ultimately leads to activation of JAK1/2 and consequent phosphorylation of the transcription factor STAT3. The phosphoform of STAT3 translocates to the nucleus to facilitate the transcription of IL-6 target genes such as *HAMP* [50,51]. In the present study, we have shown not only the upregulation of IL-6 at the mRNA and protein levels but also the increased expression of the phosphoform of STAT3 in the matriptase-2 knockout mouse retina. Although these studies convincingly show that the upregulation of hepcidin expression in the matriptase-2 knockout mouse retina occurs most likely via IL-6, the relationship between iron deficiency observed in this mouse and increased IL-6 production in the retina remains to be explored at the molecular level.

ACKNOWLEDGMENTS

This work was supported by NEI grant R01EY019672.

REFERENCES

1. Lee PL, Beutler E. Regulation of hepcidin and iron-overload disease. Annu Rev Pathol 2009; 4:489-515. [PMID: 19400694].
2. Ganz T, Nemeth E. Hepcidin and iron homeostasis. Biochim Biophys Acta 2012; 1823:1434-43. [PMID: 22306005].
3. Park CH, Valore EV, Waring AJ, Ganz T. Hepcidin, a urinary antimicrobial peptide synthesized in the liver. J Biol Chem 2001; 276:7806-10. [PMID: 11113131].
4. De Domenico I, Ward DM, Kaplan J. Hepcidin and ferroportin: the new players in iron metabolism. Semin Liver Dis 2011; 31:272-9. [PMID: 21901657].

5. Ganz T. Macrophages and systemic iron homeostasis. J Innate Immun 2012; 4:446-53. [PMID: 22441209].
6. Fuqua BK, Vulpe CD, Anderson GJ. Intestinal iron absorption. J Trace Elem Med Biol 2012; 26:115-9. [PMID: 22575541].
7. Hentze MW, Muckenthaler MU, Galy B, Camaschella C. Two to tango: regulation of mammalian iron metabolism. Cell 2010; 142:24-38. [PMID: 20603012].
8. Kaplan J, Ward DM, De Domenico I. The molecular basis of iron overload disorders and iron-linked anemias. Int J Hematol 2011; 93:14-20. [PMID: 21210258].
9. Drakesmith H, Prentice AM. Hepcidin and the iron-infection axis. Science 2012; 338:768-72. [PMID: 23139325].
10. Lin L, Glodberg YP, Ganz T. Competitive regulation of hepcidin mRNA by soluble and cell-associated hemojuvelin. Blood 2005; 106:2884-9. [PMID: 15998830].
11. Silvestri L, Pagani A, Camaschella C. Furin-mediated release of soluble hemojuvelin: a new link between hypoxia and iron homeostasis. Blood 2008; 111:924-31. [PMID: 17938254].
12. Wang RH, Li C, Xu X, Zheng Y, Xiao C, Zerfas P, Cooperman S, Eckhaus M, Rouault T, Mishra L, Deng CX. A role of SMAD4 in iron metabolism through the positive regulation of hepcidin expression. Cell Metab 2005; 2:399-409. [PMID: 16330325].
13. Babitt JL, Huang FW, Wrighting DM, Xia Y, Sidis Y, Samad TA, Campagna JA, Chung RT, Schneyer AL, Woolf CJ, Andrews NC, Lin HY. Bone morphogenetic protein signaling by hemojuvelin regulates hepcidin expression. Nat Genet 2006; 38:531-9. [PMID: 16604073].
14. Babitt JL, Huang FW, Xia Y, Sidis Y, Andrews NC, Lin HY. Modulation of bone morphogenetic protein signaling in vivo regulates systemic iron balance. J Clin Invest 2007; 117:1933-9. [PMID: 17607365].
15. Verga Falzacappa MV, Vujic Spasic M, Kessler R, Stolte J, Hentze MW, Muckenthaler MU. STAT3 mediates hepatic hepcidin expression and its inflammatory stimulation. Blood 2007; 109:353-8. [PMID: 16946298].
16. Sun CC, Vaja V, Babitt JL, Lin HY. Targeting the hepcidin-ferroportin axis to develop new treatment strategies for anemia of chronic disease and anemia of inflammation. Am J Hematol 2012; 87:392-400. [PMID: 22290531].
17. He X, Hahn P, Iacovelli J, Wong R, King C, Bhisitkul R, Massaro-Giordano M, Dunaief JL. Iron homeostasis and toxicity in retinal degeneration. Prog Retin Eye Res 2007; 26:649-73. [PMID: 17921041].
18. Gnana-Prakasam JP, Martin PM, Simth SB, Ganapathy V. Expression and function of iron-regulatory proteins in retina. IUBMB Life 2010; 62:363-70. [PMID: 20408179].
19. Martin PM, Gnana-Prakasam JP, Roon P, Smith RG, Smith SB, Ganapathy V. Expression and polarized localization of the hemochromatosis gene product *HFE* in retinal pigment epithelium. Invest Ophthalmol Vis Sci 2006; 47:4238-44. [PMID: 17003411].
20. Gnana-Prakasam JP, Zhang M, Martin PM, Atherton SS, Smith SB, Ganapathy V. Expression of the iron-regulatory protein haemojuvelin in retina and its regulation during cytomegalovirus infection. Biochem J 2009; 419:533-43. [PMID: 19191760].
21. Gnana-Prakasam JP, Martin PM, Mysona BA, Roon P, Smith SB, Ganapathy V. Hepcidin expression in mouse retina and its regulation via lipopolysaccharide/Toll-like receptor-4 pathway. Biochem J 2008; 411:79-88. [PMID: 18042040].
22. Hadziahmetovic M, Song Y, Ponnuru P, Iacovelli J, Hunter A, Haddad N, Beard J, Connor JR, Vaulont S, Dunaief JL. Age-dependent retinal iron accumulation and degeneration in hepcidin knockout mice. Invest Ophthalmol Vis Sci 2011; 52:109-18. [PMID: 20811044].
23. Hahn P, Milam AH, Dunaief JL. Maculas affected by age-related macular degeneration contain increased chelatable iron in the retinal pigment epithelium and Bruch's membrane. Arch Ophthalmol 2003; 121:1099-105. [PMID: 12912686].
24. Dunaief JL, Richa C, Franks EP, Schultze RL, Aleman TS, Schenck JF, Zimmerman EA, Brooks DG. Macular degeneration in a patient with aceruloplasminemia, a disease associated with retinal iron overload. Ophthalmology 2005; 112:1062-5. [PMID: 15882908].
25. Hahn P, Quan Y, Dentchev T, Chen L, Beard J, Harris ZL, Dunaief JL. Disruption of ceruloplasmin and hephaestin in mice causes retina iron overload and retinal degeneration with features of age-related macular degeneration. Proc Natl Acad Sci USA 2004; 101:13850-5. [PMID: 15365174].
26. Hadziahmetovic M, Dentchev T, Song Y, Haddad N, He X, Hahn P, Pratico D, Wen R, Harris ZL, Lambris JD, Beard J, Dunaief JL. Ceruloplasmin/hephaestin knockout mice model morphologic and molecular features of AMD. Invest Ophthalmol Vis Sci 2008; 49:2728-36. [PMID: 18326691].
27. Gnana-Prakasam JP, Thangaraju M, Liu K, Ha Y, Martin PM, Smith SB, Ganapathy V. Absence of iron-regulatory protein *Hfe* results in hyperpolarization of retinal pigment epithelium: role of cystine/glutamate exchanger. Biochem J 2009; 424:243-52. [PMID: 19715555].
28. Gnana-Prakasam JP, Ananth S, Prasad PD, Zhang M, Atherton SS, Martin PM, Smith SB, Ganapathy V. Expression and iron-dependent regulation of the succinate receptor GPR91 in retinal pigment epithelium. Invest Ophthalmol Vis Sci 2011; 52:3751-8. [PMID: 21357408].
29. Gnana-Prakasam JP, Tawfik A, Romej M, Ananth S, Martin PM, Smith SB, Ganapathy V. Iron-mediated retinal degeneration in haemojuvelin-knockout mice. Biochem J 2012; 441:599-608. [PMID: 21943374].
30. Ramsay AJ, Hooper JD, Folgueras AR, Velasco G, Lopez-Otin C. Matriptase-2 (TMPRSS6): a proteolytic regulator of iron homeostasis. Haematologica 2009; 94:840-9. [PMID: 19377077].
31. Lee P. Role of matriptase-2 (TMPRSS6) in iron metabolism. Acta Haematol 2009; 122:87-96. [PMID: 19907145].

32. Silvestri L, Pagani A, Nai A, De Domenico I, Kaplan J, Camaschella C. The serine protease matriptase-2 (TMPRSS6) inhibits hepcidin activation by cleaving membrane hemojuvelin. Cell Metab 2008; 8:502-11. [PMID: 18976966].

33. Finberg KE. Iron-refractory iron deficiency anemia. Semin Hematol 2009; 46:378-86. [PMID: 19786206].

34. Camaschella C, Poggiali E. Inherited disorders of iron metabolism. Curr Opin Pediatr 2011; 23:14-20. [PMID: 21150441].

35. Du X, She E, Gelbart T, Truksa J, Lee P, Xia Y, Khovananth K, Mudd S, Mann N, Moresco EM, Beutler E, Beutler B. The serine protease TMPRSS6 is required to sense iron deficiency. Science 2008; 320:1088-92. [PMID: 18451267].

36. Umapathy NS, Li W, Mysona BA, Smith SB, Ganapathy V. Expression and function of glutamine transporters SN1 (SNAT3) and SN2 (SNAT5) in retinal Muller cells. Invest Ophthalmol Vis Sci 2005; 46:3980-7. [PMID: 16249471].

37. Dun Y, Mysona B, Van Ells T, Amarnath L, Ola MS, Ganapathy V, Smith SB. Expression of the cystine-glutamate exchanger (x_c^-) in retinal ganglion cells and regulation by nitric oxide and oxidative stress. Cell Tissue Res 2006; 324:189-202. [PMID: 16609915].

38. Martin PM, Dun Y, Mysona B, Ananth S, Roon P, Smith SB, Ganapathy V. Expression of the sodium-coupled monocarboxylate transporters SMCT1 (SLC5A8) and SMCT2 (SLC5A12) in retina. Invest Ophthalmol Vis Sci 2007; 48:3356-63. [PMID: 17591909].

39. Enns CA, Ahmed R, Zhang A. Neogenin interacts with matriptase-2 to facilitate hemojuvelin cleavage. J Biol Chem 2012; 287:35104-17. [PMID: 22893705].

40. Gnana-Prakasam JP, Reddy SK, Veeranan-Karmegam R, Smith SB, Martin PM, Ganapathy V. Polarized distribution of heme transporters in retinal pigment epithelium and their regulation in the iron-overload disease hemochromatosis. Invest Ophthalmol Vis Sci 2011; 52:9279-86. [PMID: 22058337].

41. Velasco G, Cal S, Quesada V, Sanchez LM, Lopez-Otin C. Matriptase-2, a membrane-bound mosaic serine proteinase predominantly expressed in human liver and showing degrading activity against extracellular matrix proteins. J Biol Chem 2002; 277:37637-46. [PMID: 12149247].

42. Hooper JD, Campagnolo L, Goodarzi G, Truong TN, Stuhlmann H, Quigley JP. Mouse matriptase-2: identification, characterization and comparative mRNA expression analysis with mouse hepsin in adult and embryonic tissues. Biochem J 2003; 373:689-702. [PMID: 12744720].

43. Knutson MD. Into the matrix: regulation of the iron regulatory hormone hepcidin by matriptase-2. Nutr Rev 2009; 67:284-8. [PMID: 19386032].

44. Zhang AS, Anderson SA, Wang J, Yang F, DeMaster K, Ahmed R, Nizzi CP, Eisenstein RS, Tsukamoto H, Enns CA. Suppression of hepatic hepcidin expression in response to acute iron deprivation is associated with an increase of matriptase-2 protein. Blood 2011; 117:1687-99. [PMID: 21115976].

45. Meynard D, Vaja V, Sun CC, Corradini E, Chen S, López-Otín C, Grgurevic L, Hong CC, Stirnberg M, Gütschow M, Vukicevic S, Babitt JL, Lin HY. Regulation of TMPRSS6 by BMP6 and iron in human cells and mice. Blood 2011; 118:747-56. [PMID: 21622652].

46. Finberg KE, Whittlesey RL, Fleming MD, Andrews NC. Down-regulation of Bmp/Smad signaling by Tmprss6 is required for maintenance of systemic iron homeostasis. Blood 2010; 115:3817-26. [PMID: 20200349].

47. Lenoir A, Deschemin JC, Kautz L, Ramsay AJ, Roth MP, Lopez-Otin C, Vaulont S, Nicolas G. Iron-deficiency anemia from matriptase-2 inactivation is dependent on the presence of functional Bmp6. Blood 2011; 117:647-50. [PMID: 20940420].

48. Finberg KE, Whittlesey RL, Andrews NC. Tmprss6 is a genetic modifier of the *Hfe*-hemochromatosis phenotype in mice Blood 2011; 117:4590-9. [PMID: 21355094].

49. Krijt J, Fujikura Y, Ramsay AJ, Velasco G, Nečas E. Liver hemojuvelin protein levels in mice deficient in matriptase-2 (Tmprss6). Blood Cells Mol Dis 2011; 47:133-7. [PMID: 21612955].

50. Wrighting DM, Andrews NC. Interleukin-6 induces hepcidin expression through STAT3. Blood 2006; 108:3204-9. [PMID: 16835372].

51. Sun CC, Vaja V, Babitt JL, Lin HY. Targeting the hepcidin-ferroportin axis to develop new treatment strategies for anemia of chronic disease and anemia of inflammation. Am J Hematol 2012; 87:392-400. [PMID: 22290531].

Articles are provided courtesy of Emory University and the Zhongshan Ophthalmic Center, Sun Yat-sen University, P.R. China. The print version of this article was created on 26 April 2014. This reflects all typographical corrections and errata to the article through that date. Details of any changes may be found in the online version of the article.